DOI: 10.13009/EUCASS2017-632



# On Ground Validation of Debris Removal technologies

*P. Colmenarejo*, M. Graziano*, G. Novelli*, D. Mora*, P. Serra*, A. Tomassini**
*K. Seweryn***
*G. Prisco****
*J. Gil Fernandez*****
**GMV, Isaac Newton, 11, 28760 Tres Cantos, Madrid, Spain*
***CBK PAN, Warsaw, Poland*
****TSD, Naples, Italy*
*****ESA/ESTEC, Noordwijk, Netherland*

## Abstract
The situation of orbital debris is becoming more and more a worldwide concern for the safe operations of space assets. In this context, retiring orbital debris (and extending life or repairing damaged on-orbit assets) is very attractive to satellite operators as it could potentially decrease mission risks, increase margins for commercial services or increase delivered value of scientific missions).
Debris removal services (also in-orbit servicing and in-orbit assembly) require combined operation of different critical technologies, mainly autonomy, manipulation robotics, spacecraft GNC and vision-based navigation/image processing. A full combined/coupled sequence involving those critical technologies has never been performed in–orbit and has also never been tested comprehensively on ground.
GMV has led a consortium (completed with Polish CBK institute for advanced space robotics manipulator solutions and with Italian TSD company with visual-based HW heritage) that has performed an ESA funded activity with the objective of advancing and exercising with real HW in the loop (HIL) and using a space-representative dynamic laboratory the referred key technologies required to perform complex robotic scenarios needing a rigid capture mechanism such as a robotic arm.
The final goal of this activity (On-ground Validation of Debris Removal Technologies, ORCO) has been to investigate and mature the complex couplings between the different control systems (GNC including image processing and robotics) for autonomous rigid capture between an active chaser vehicle and a cooperative/non-cooperative target, and derive the required algorithms and perform a HW-in-the-loop end-to-end demonstration. The prototyped solution is tested in the most realistic conditions obtainable on ground, including also the dynamics of the system as well as the relative visual based navigation system. The on-ground validation and integration is performed taking advantage of the GMV ***platform-art***© dynamic test facility located in Madrid, Spain, with the addition of the hardware provided by the partners: robotic system from CBK (Poland) and visual system from TSD (Italy).
Ultimately, the consortium has achieved the objective of performing a comprehensive ground testing of all abovementioned critical technologies for debris removal missions, thus contributing to the technologies maturation and to the de-risking of future implementations and testing. Particularly relevant is the availability of a HIL dynamic based laboratory ready to host and test evolved or new debris removal solutions quickly and with a high degree of space representativeness.
Based on the obtained results, firstly based on pure SW-based simulations and ultimately verified/validated based on HIL dynamic laboratory tests, this paper includes system level considerations (e.g. analysis and recommendations at mission/system level derived from the performed tests), and subsystem results and recommendations (e.g. best image processing/visual-based system set-up/combination depending on the debris removal scenario phase, target size/characteristics, etc; best/safe guidance trajectories to approach a non-cooperative target; combined operations of chaser spacecraft GNC and robotic manipulator control system; autonomy issues such as GNC modes transitions and autonomous navigation; etc).

DOI: 10.13009/EUCASS2017-632



## 1. Introduction

One of the main drawbacks of space systems is the strong reliability and robustness requirements they must comply with, as there is currently no real possibility of repairing in-orbit assets (with few notable exceptions, such as the costly refurbishing of the Hubble telescope by Space Shuttle NASA mission). The potential of having an in-orbit service has been discussed since many years; however this has never been translated into a reality because of the high cost and the technical complexities and low TRL of the required systems. Recently however there has been a return of interest in the in-orbit servicing potential, notable examples can be cited within Europe with the DLR servicing DEOS mission (technical demonstrator for servicing) and the current ESA-sponsored ASSIST activity (hArmonised System Study on Interfaces and Standardisation of fuel Transfer, [3]). Both initiatives are focused at developing enabling technologies for servicing missions, but no end-to-end system demonstration has been carried out so far.
In parallel, it has been gaining momentum in the space community the necessity of having modular spacecraft that can be assembled in orbit using autonomous robots: such systems will enable new concepts such as the DLR's iBoss (Intelligent Building Blocks for On-Orbit Satellite Servicing, [4]) or FLEXSAT concept introduced by the H2020 PERASPERA ESA-led project (robotics servicing technology aiming a composable, reconfigurable and refuelable spacecraft, [5]), which would be game changer in the way we build, launch, operate and dispose assets in orbit. More into the medium term future, in orbit assembly has also been proposed for larger exploration missions (human missions) or the assembly of large structures in low earth orbit like refuelling stations or solar power satellites.
Also, space debris remediation technologies are being currently developed in order to enable an active debris removal mission. The DEOS mission and the eDeorbit activities within ESA's CleanSpace initiative have identified the capture with a robotic arm as one the most promising (and flexible) capture technology for Active Debris Removal missions.
All of the above applications have identified robotics as one of their enabling technologies. In particular, all of them will need the manipulation of a man-made object (being an element to be assembled, an active satellite or a space debris) using a robotic arm from an active "chaser" satellite that will have to perform rendez-vous with a passive "client" navigating autonomously, grab the client that has to be assumed in a non-controlled state (worst case) and then control the "combo" composed by the chaser and the client connected by a robotic arm. The complexity of such tasks are various: the uncertainties in the knowledge of the client object, the autonomy of the operations, the control of the robotic arm during deployment and grasping and, finally, the control of the combo with a rigid link. In fact, this has been all identified by the H2020 PERASPERA project (which includes all major robotic players in Europe) as required technologies to allow in-orbit repair and the modular satellite concept.
This sequence (and strong interrelation) of autonomous relative navigation, capture of the client and control of the combo has never been performed in–orbit and has also never been tested comprehensively on ground including the major system elements (i.e. autonomy, robotic system, GNC and visual navigation). Solving this complex technological challenge requires state-of-the art expertise in each of the mentioned areas and a system approach to solve the technical complexities that arise from their interrelations. Within ORCO project a full iteration of the major elements of such complex system has been made, performing the required investigations on the control approach including the interactions of the spacecraft and robotics control system and performing an end-to-end on-ground demonstration of the proposed solution using ***platform-art*©** dynamic test bench.

## 2. Reference Mission scenario

The AnDROiD mission ([1], [2]) has been taken as reference mission for the ORCO scenario description, covering both targeted in-orbit servicing (IOS) and active debris removal (ADR) scenarios. AnDROiD mission (developed till a "preliminary definition" level by GMV, Qinetiq and CBK PAN within an ESA funded study), includes most of the elements that have been identified as target of ORCO project. AnDROiD mission architecture is composed by:

- Single chase spacecraft equipped with robotic arm, net system (not applicable to ORCO) and GNC equipment for rendezvous, capture and deorbit
- Launch with VEGA – VESPA (single passenger, TBC)
- Dry mass 279 kg (including margins); Propellant mass 68 kg; Total mass at launch 353 kg (including launcher I/F ring)
- Dimensions 1188 (D) x 1133 (W) x 1145(H) mm
- Total DV 399 m/s (including margins)
- High level of autonomy of the system for almost all phases except for orbit synchronisation. AnDROiD mission timeline as shown in Figure 2.
- AnDROiD mission target is PROBA2 satellite (also considered as target for ORCO activity too). PROBA2 is a real example of a real space debris. PROBA2 was launched in 2009 into a LWO 718km sunsynchronous orbit with and inclination of 98.28deg and LTAN of 06h24 am.

DOI: 10.13009/EUCASS2017-632



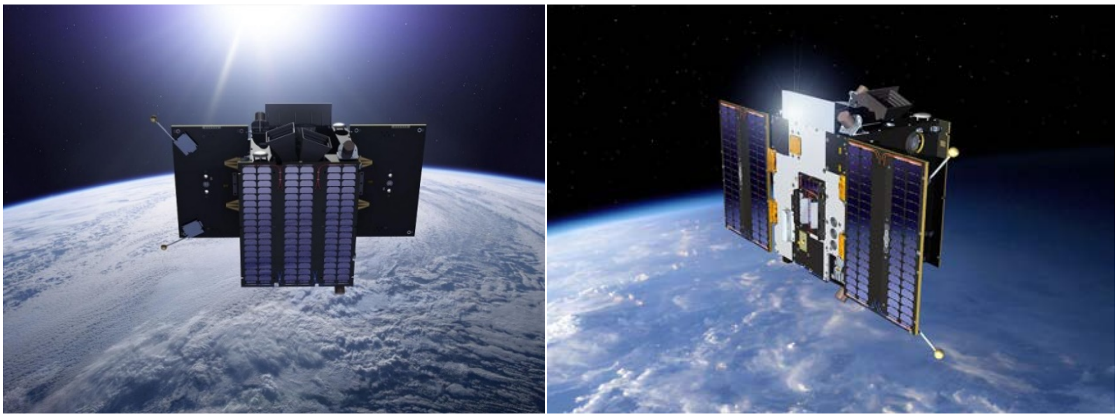

Figure 1: Artist's impression of PROBA 2

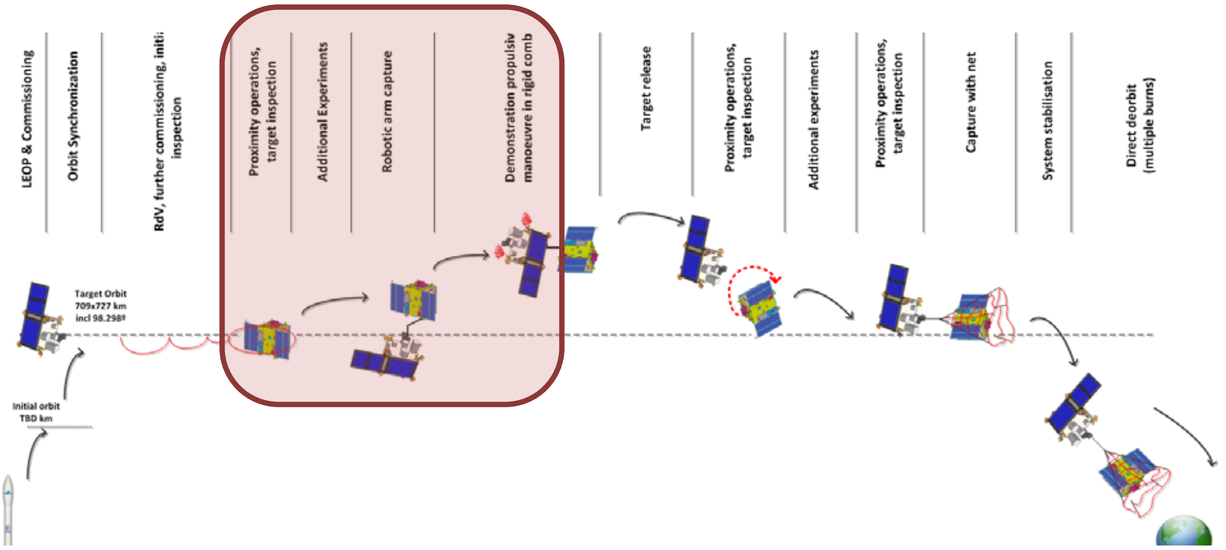


Figure 2 AnDROiD mission timeline and phases (red shadowed) considered within ORCO

The rendezvous, final approach and capture phases of AnDROiD mission are hereafter described because of the relevance to ORCO scenario. The rendezvous strategy is based on drifting trajectories and the safe orbit described above. Rendezvous starts at a distance of about 2000 m behind the target and 500 m below. This location is labelled as S1. At this point the chaser starts modulating its drift rate while maintaining the relative apogee at 50 m below the target orbit. This sequence occurs between points S2a and S4. All manoeuvres "a" have the objective to modify relative perigee, and manoeuvres labelled "b" are intended to modify relative apogee. Out-of-plane control can be performed at either "a" or "b". At point S4 the chaser enters into a co-elliptic drift orbit 50 m below the target, and at point S5 the chaser enters into a safe orbit with a closest along-track approach distance of about 100 m (this means that the centre of the safe orbit ellipse is located at an along-track distance of about 200 m.)

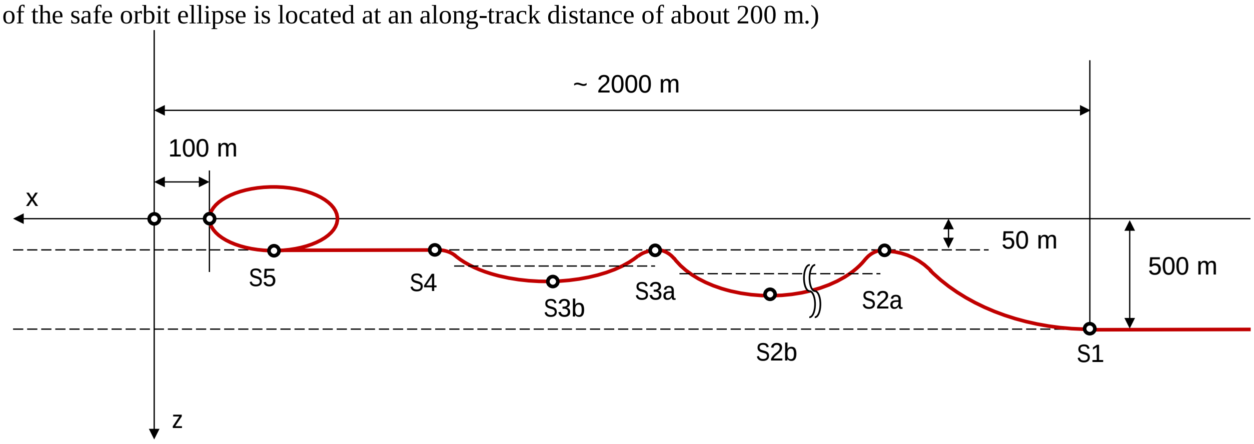


Figure 3 AnDROiD rendezvous strategy

DOI: 10.13009/EUCASS2017-632



Figure 4 shows a forced motion approach trajectory to be used during the close range proximity operations. At point S1 the out-of-plane motion associated with the safe orbit is removed. At point S2 a radial manoeuvre is performed to put the chaser into a hold point on V-bar. Between points S2 and S3 a forced motion approach is performed.

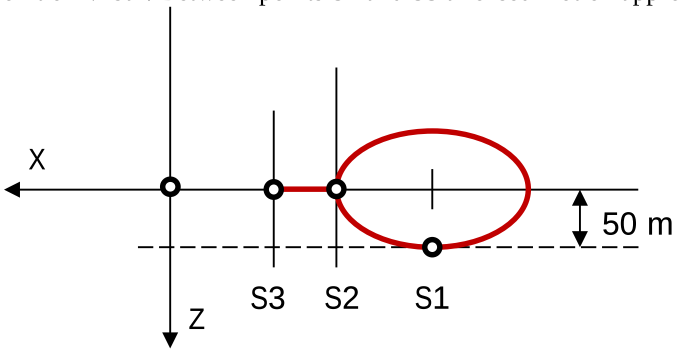


Figure 4: Close range forced motion trajectory

The following set of proximity operations are then performed:
1. Approach in target body fixed frame including angular synchronization
2. Capture with robotic arm
3. Stabilisation

The approach/angular synchronization in the target body fixed frame requires continuous thrust acceleration (i.e., forced motion trajectories) and occurs below a distance of 20 metres. The approach in the target body fixed frame is considered proximity operations. Figure 5 shows several approach strategies for approaching a spinning satellite, labelled A, B and C. The base reference frame of the figure is the LVLH frame, but certain parts of the trajectory are performed in other reference frames, such as the inertial reference frame or in the target body reference frame.

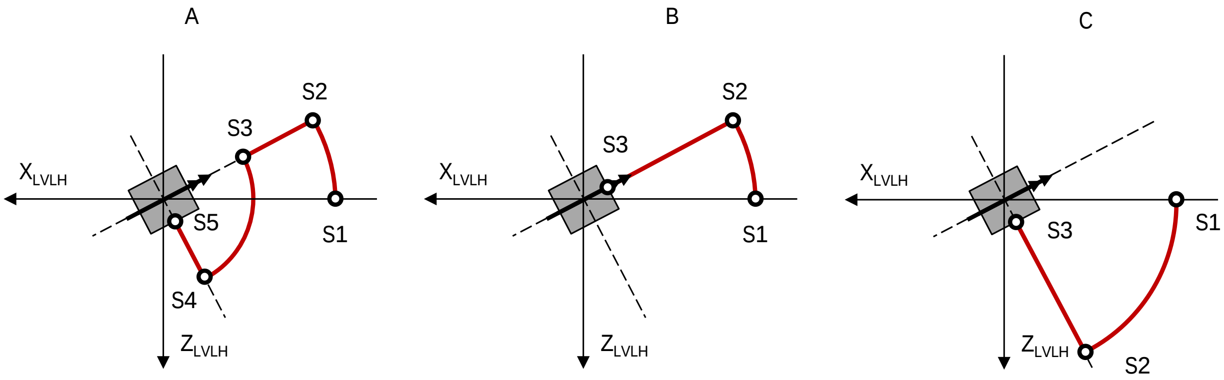


Figure 5: Proximity operations for a spinning satellite

Strategy A consists of the following elements:
- S1 to S2: Fly-around to a point on the body spin-axis
- S2 to S3: Perform straight-line approach over spin axis
- S3 to S4: Fly-around in target body fixed frame to grasping point
- S4 to S5: Perform straight-line forced motion to grasping point contact

Strategy A is designed for a fast spinning satellite. If the debris object is spinning fast, it will be costly to maintain a position perpendicular to the spin axis of the body, because the centrifugal acceleration needs to be compensated for by the thrusters. So if the target object is spinning fast it may be necessary to perform a first approach over the spin axis of the body to get fairly close to the target, followed by a fly-around to the grasping that is as short as possible to save propellant.

Strategy B and C are simplifications of strategy A. In strategy B, the debris object is grasped at a point on or very close to the spin axis of the body. In strategy C, the chaser performs a fly-around in the LVLH frame to the expected location of the projection of the approach direction on a sphere with radius 20 m at S2. At S2, the chaser starts following the approach direction in the objects body frame and performs the approach to the target object from S2 to S3 in the target body frame.

DOI: 10.13009/EUCASS2017-632



### 2.1 ORCO Scenarios

Based on the AnDROiD mission definition provided in previous section, the following scenarios have been derived to analyse, mature and validate the most relevant involved technologies:

1. Cooperative target (Servicing scenario): representative of a servicing/assembly mission where the target is fully cooperative, i.e. its attitude is controlled and can provide navigation aids (rGPS, reflectors, etc). This scenario is the most favourable both from the point of view of the GNC and the robotic arm control. In this case the visual system is assumed to be a redundant system to be used for off nominal situations like collision risk detection. The chaser will approach the target along Vbar performing a forced motion till the final capture point. Initial distance: 10 m. Target spin rate: 0 deg/s.

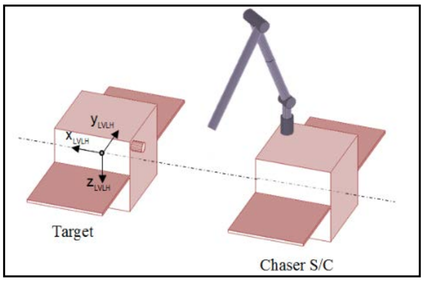


2. Non-cooperative target with slow rotation (no synchronization): representative of an active debris removal mission where the target is small enough or its spin rate is slow enough for the system to perform the capture without the need of reducing residual velocities between the target and the chaser to the minimum, that is, the robotic arm is capable of dealing with this differences. This would be the most complex case for the robotic arm. Initial distance: 10 m. Target spin rate: 0.3 deg/s (PROBA2 maximum expected spin rate).

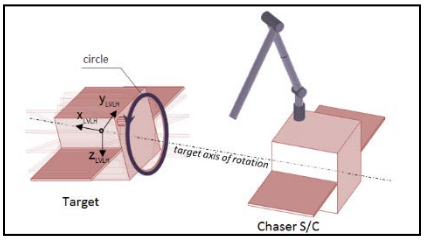


3. Non-cooperative tumbling target with spin synchronization: representative of an active debris removal mission for a large target. In this case the residual velocities (linear and angular) are reduced to zero plus control errors), making the capture by the robotic arm similar to the scenario 1. This will be the most demanding scenario for the GNC, as spin synchronisation with the target will be required to eliminate relative velocities. Initial distance: 10 m. Target spin rate: 3.5 deg/s (12 times worse than AnDROiD/PROBA2 worst case and similar to ENVISAT current spinning rate).

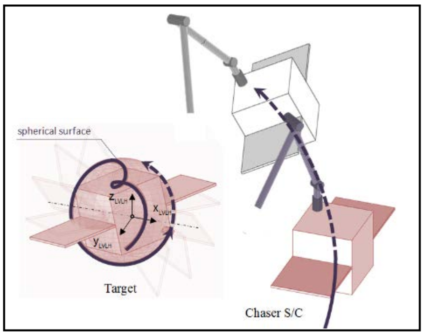


## 3. Control System Architecture and Development Approach

Figure 6 shows the overall view of the high level SW/HW bricks constituting the ORCO Control System that allows performing the different phases of the mission: approach/synchronisation, station keeping, manipulator operations, and contact phase.

The three main SW/HW elements/subsystems are:

- Chaser spacecraft GNC
- LEMUR robotic space manipulator and control sub-system
- Relative navigation camera system (including image processing)

There will be two validation levels:

- SW-level based on Model-in-The-Loop Matlab/Simulink simulator, that needs for the simulation of DKE (Dynamics, Kinematics and Environment) models + sensors models + actuators models (bottom part of Figure 6).
- HW-level based on HW-in-The-Loop laboratory (***platform-art***©) that includes real dynamics provided by KUKA commercial robotic devices (fed with the relative chaser-target spacecraft state computed by the DKE SW models) hosting target spacecraft physically-representative mockup, force/torque measurements cells, realistic illumination conditions provided by dedicated Sun-like numerically controlled Sun emulator. All together providing realistic air-to-air stimulation of relevant sensors (navigation camera), and everything under real-time system (dSpace system) and space-representative processors (e.g. Leon family, Virtex5).

The three SW bricks will be hosted and executed in separated processors:

DOI: 10.13009/EUCASS2017-632



- The Chaser OBSW/GNC on the spacecraft Main Computer (OBC)
- The LEMUR controller on a dedicated control board (LEMUR Control Board)
- The optical navigation algorithms on a dedicated FPGA system (HPVN)

These are the three main elements/sub-systems that have been iterated and matured during ORCO activity. The following sections provide details on each of them.

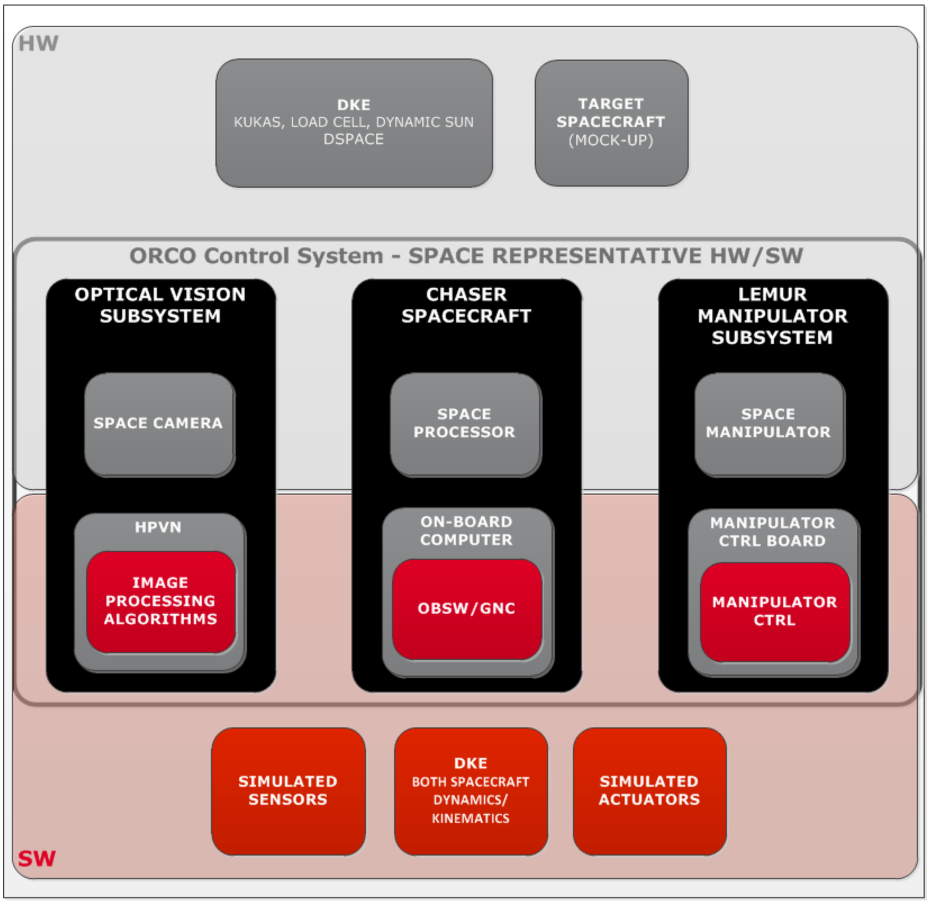


Figure 6: ORCO Control System, HW and SW bricks

## 4. Chaser spacecraft GNC System

Figure 7 shows as a diagram the main bricks constituting the spacecraft OBSW (On Board SW) with a special focus on the GNC architecture and its several I/F and relations with other elements of the ORCO Control System. As it can be seen the GNC is made up of 7 functions:

1. Navigation: it provides the on-board estimation of 1) the absolute chaser state, 2) the relative chaser translational state of the chaser wrt target in LVLH (Local Vertical Local Horizontal) frame and 3) the absolute estimation of the target attitude state. It is fed by the Chaser sensors suite and in particular by the image processing solutions.
2. Guidance: given the navigation data, this function delivers the desired reference trajectory (attitude, angular rate, position and velocity) and the reference feed-forward forces and torques signal for the different mission phases.
3. Control: this function implements the digital robust control for the Chaser spacecraft system.
4. Multibody System Configuration: a service module providing information about the on-board knowledge of MCI properties of the multibody system and End-Effector kinematic state wrt Chaser Body Frame; it uses the manipulator joint angles and angles rates coming from the LEMUR board.
5. Navigation for LEMUR operations: given the multibody kinematics, it provides the estimation of the chaser spacecraft centre of mass (only base, not including the arm) relative state wrt the target in LVLH and Target body frame, as well as the complete LEMUR end-effector kinematic state wrt Target Body Frame, thus acting as the “eye” of the LEMUR subsystem.

DOI: 10.13009/EUCASS2017-632



6. IP Service Module: a service module providing to camera/image processing subsystem all the needed information to work properly; time synchronisation and image sampling signals, estimation of the Sun direction in camera frame, a-priori estimation of the target relative pose (to be used as initialization aid by the IP algorithms and for estimation of the level of uncertainty on the IP solutions).
7. LEMUR Trajectory: this function uses data from a reference LEMUR trajectory pre-computed on ground, and received by the TMTC chaser system; it is in charge of interpolating the trajectory through usage Look-up-tables and sending it to the LEMUR controller during the catching operations phase.

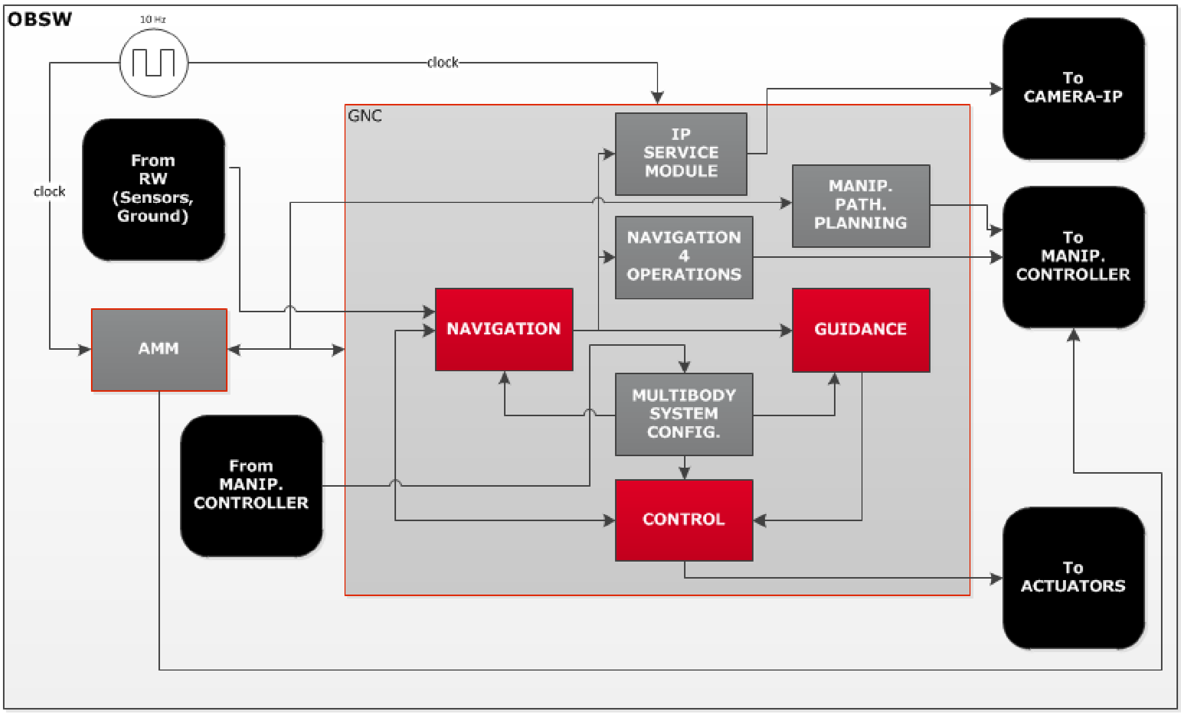


Figure 7: Chaser spacecraft GNC architecure and its interfaces with other OBSW elements

## 5. Visual-based Navigation

### 5.1 Image Processing algorithms

For the observation and synchronization phases we decided that the Model Based Tracking was the best option, mainly because of its robustness to illumination but also because of its ability to recover from small pose approximation errors (meaning that even after a non-perfect initialization or a frame where for any reason the computed pose was not perfect, because of its 'absolute' behaviour, the MBT does not start to drift away from the correct solution, but instead, self-corrects adjusting the edges of the model on the image).
Still, it was thought that in the final phase, it was possible that the camera would be too close to the target in order to see enough edges properly to compute the pose. Therefore we wanted another approach for this phase as a backup.
In the final phase, the target is supposed to be quite static, and the chaser is close enough to the target that the camera can see the texture of the target surface. In these conditions, a tracking based on interest points could work and be stable, so the KLT (Kanade-Lucas-Tomasi feature tracker) algorithm was decided to be implemented as well for the final phase.

The Model Based Tracking scheme is suitable for poorly textured targets (from which we know their geometry) with good visible salient edges that can be tracked, on the other hand, KLT does not need to know a priori the geometry of the target to be tracked, but it relies on its texture.
Once the mock-up arrived to the ***platform-art©*** and real images with space-representative illumination were acquired, it was realised that the images appeared more textured than it was thought (in theory) they would be. This effect is mainly caused by the so different properties of light reflexion of the surfaces involved. In the end the result is that the supposedly salient edges are not that evident to the camera, and on the other hand there are planar surfaces that because

DOI: 10.13009/EUCASS2017-632



of the different materials in which they are divided, they show some clear separation between them. This means that it was not difficult that some salient edge searched by the algorithm was in fact matched to some 'apparent' new internal fake edge that was actually a boundary between different materials (see Figure 8).

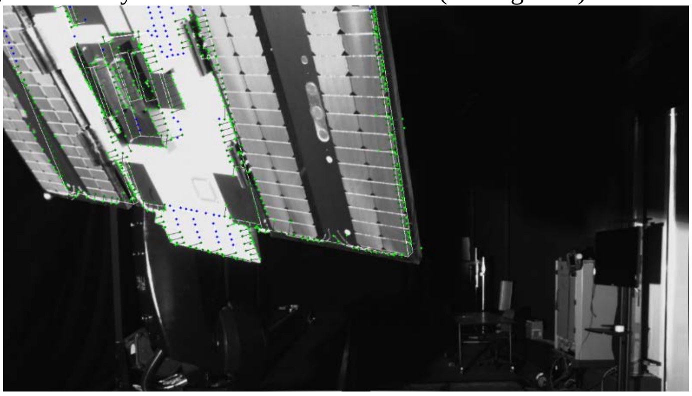

Figure 8: Poor edge tracking due to a textured surface

To overcome this issues it was thought how we could get the best from both KLT and edge-MBT due to the fact that our realistic target mockup is halfway between a highly textured target and an edge based one (this is the real expected situation to have in orbit).

Then, our approach has been using the KLT where it excels the MBT, in the frame-to-frame transformation, and use the MBT where it excels the KLT, in the absolute computation of the relative pose between target and chaser.

Adding all up, for every new frame we divide the computation in two steps:

- First step: the KLT computes a frame-to-frame relative transformation. Basically it tracks texture features from the previous image to the actual one, but to compute the rigid transformation, it retro-projects the features from the previous frame into the previous estimated 3D pose of the target so it gets the estimated 3D position of this features. Then with their 2D coordinates in the actual frame it is possible to compute the translation and rotation from one frame to the other.
- Second step: with the previous translation and rotation estimated by KLT, we initialize the MBT algorithm and then we run it in the standard way.

The main advantages of this approach are that it is more robust to high speed maneuvers (or low frequency image acquisition) due to the really good KLT frame-to-frame robustness even on big changes, but lacking its main drawback, the absolute pose to drift over time, as on the second step the MBT really keeps edges on place (not that good relative estimation on big jumps as the KLT, but way better absolute pose over time if well initialized), not allowing the error to drift and grow over time.

### 5.2 Camera and Hardware Implementation

The Visual Navigation System Hardware is mainly composed of two parts:

- CMOS Monocular Camera provided with fixed lens
- High-performance Processing unit for Visual-based Navigation (HPVN)

The overall architecture of the hardware System is shown in Figure 9, the following sections describe in detail the subsystems.

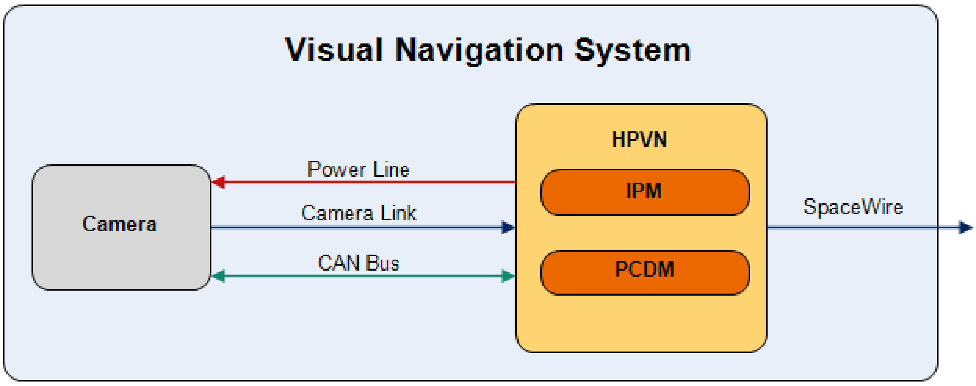


Figure 9: Visual Navigation System high level block diagram

DOI: 10.13009/EUCASS2017-632



The KLT and MBT algorithms have been FPGA accelerated using all the possible solutions offered by the methods to parallelize the operations, perform operations in pipeline, improve data access and data usage.
Figure 10 shows a high level block diagrams. There are several independent parts, the execution of which can take place in parallel. Both convolution sections have the same input, the current image, they can then work in parallel; furthermore, the KLT convolutions block perform three different kind of operation: Smooth#1 block uses as input the current image, while the Gradients#1 and Smooth#2 blocks use as input the output of Smooth#1 block. In this case, in addition to run the two blocks in parallel, the data stream can be processed as pipeline: when each pixel output of the first block is ready, it can immediately be processed simultaneously by the two successive blocks.
Subsequently, while the output of the KLT Track is calculated, the MBT Track data are prepared with the information obtained from the current image. Finally, when the KLT Track provides its output, the algorithm proceeds with MBT Track which generates the output for the current iteration, and at the same time preparing the KLT information for the next iteration.
At the end of the project the frame processing time was slightly higher than half a second. Adding half of the integration time of the image and some extra delays it means that the IP can run safely at a frequency of about 1.5Hz. It is estimated that there is still some room for acceleration improvement till, at least, working at 2Hz.

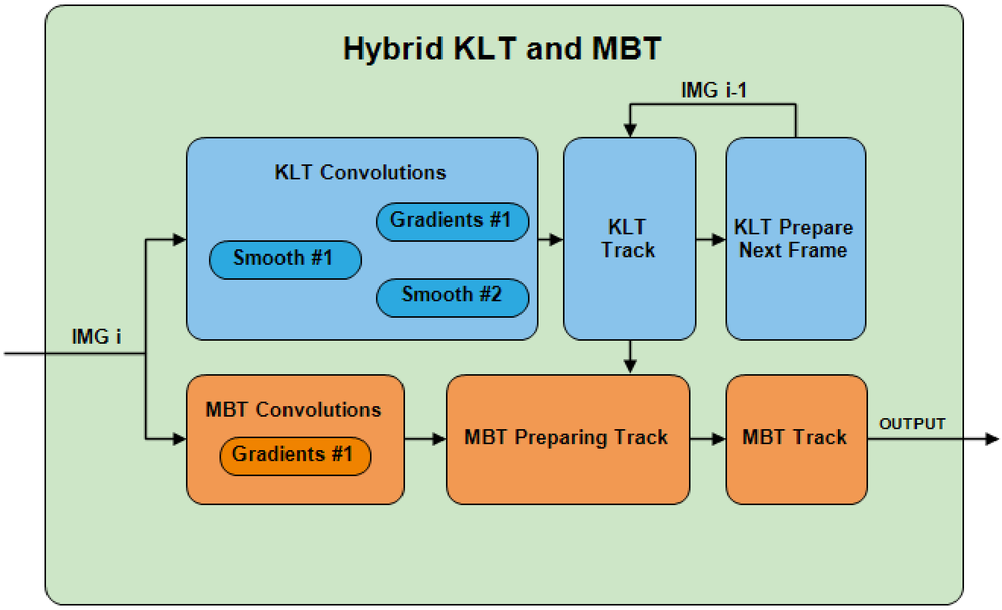

Figure 10: Hybrid KLT and MBT High Level Block Diagram

## 6. LEMUR Robotic Manipulator

In last years the manipulator arm WMS1 LEMUR was developed in CBK PAN. The laboratory model is presented on the Figure 11 (left). The system design was chosen in such way to be optimal for operation in on-orbit environment, especially for servicing operations and debris removal. The control system has three major features: path planning algorithm providing the feed forward term for controller, the singularity avoidance algorithm which takes advantage of additional joint, smoothly moves through the singularities points and made the system most robust, and control scheme which takes into account cooperation with spacecraft GNC.
In the nominal configuration the length of the laboratory model of the manipulator arm is about 3m and weight around 22kg. The manipulator has 7DoF (Degrees of Freedom), four of them dedicated to end effector positioning and remaining 3 for end effector orientations. In the final configuration dedicated for operations in space it is envisage that the mass could increase up to 40 kg. In such configuration manipulator arm cannot work in Earth gravity conditions and need to be suspended by test-bed system (also present on Figure 11 (left)).
In the frame of the ORCO project the modified version of manipulator arm (called WMS2 LEMUR, see Figure 11 right) was provided for GMV to perform the tests on platform-art facility. The manipulator arm is scaled down (4DoF, 1.3 m span) mainly because of gravity effects.

DOI: 10.13009/EUCASS2017-632



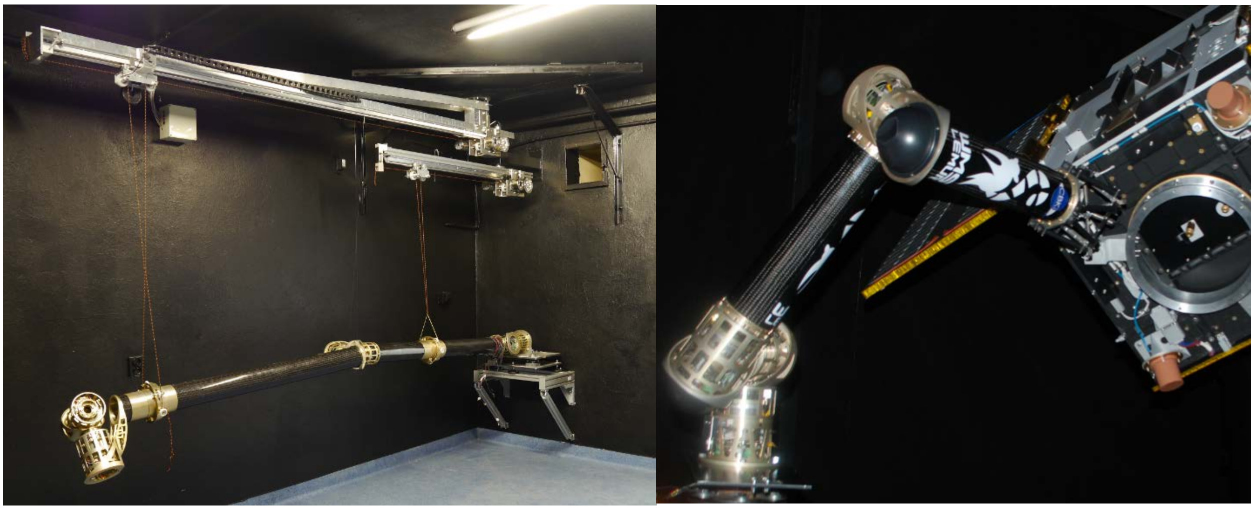

Figure 11: WMS1 LEMUR manipulator arm (left) and WMS2 manipulator for ORCO activity (right)

The control system of WMS2 Lemur arm (Figure 12) was implemented on two kinds of electronic circuits: (i) on Lemur Main Computer (LMC) and (ii) joint controllers (JC). The LMC performs trajectory control in configurational and cartesian space as well as force control and mode management. It also monitors, collects and stores all the data that comes from the executive subsystems. Control signals (reference joint angles) is calculated by LMC are sent to joint-controller boards. LMC bases on a SoM-A5D36 which is a System on Module (SoM) based on the Atmel ARM Cortex A5 ATSAMA5D36 processor. Application software and all collected data are stored on Flash and SD cards. The joint-controller circuit consists of 32bits ARM Cortex M3 microcontroller, linear power converter, set of input/output buffers and interface to communicate with the encoders. JC boards are responsible for: control of manipulator drives, monitoring positions of manipulator joints and monitoring own electronics by collecting the data about the temperatures, supply current and voltage.

Logical blocks of LEMUR computers are shown on Figure 5 8. CAN bus at 1Mbps is used for communication between LMC and joint-controllers. Special purpose CAN application level interface has been implemented on top of CAN bus to provide real time and robust transmission channel between systems nodes. It is responsible for transferring reference signals from LMC to specific joint control software and for transferring measured joint position from joint-controllers to LMC.

Due to manipulator arm requirements related to the mass mounted at end effector, a simplified contact device with a sliding steel ball has been considered and implemented (Figure 13).

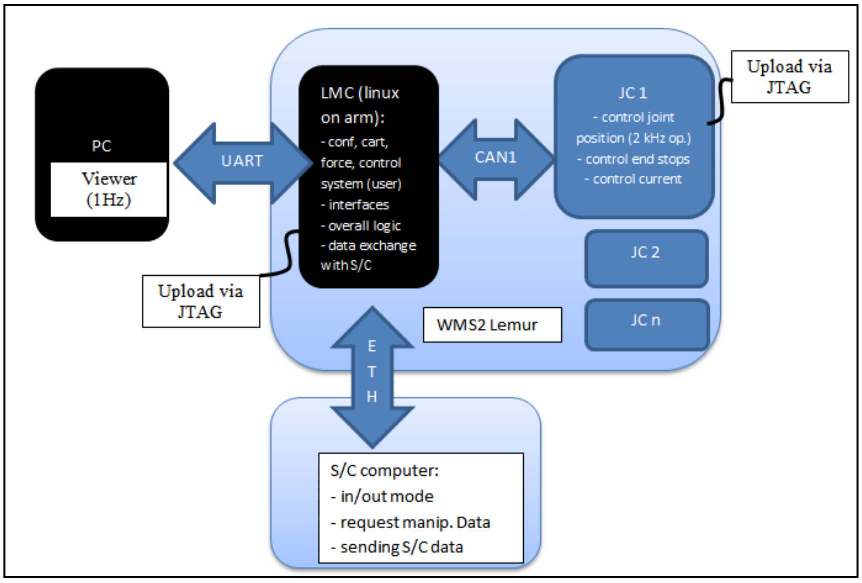


Figure 12: Logical blocks of Lemur computer

DOI: 10.13009/EUCASS2017-632



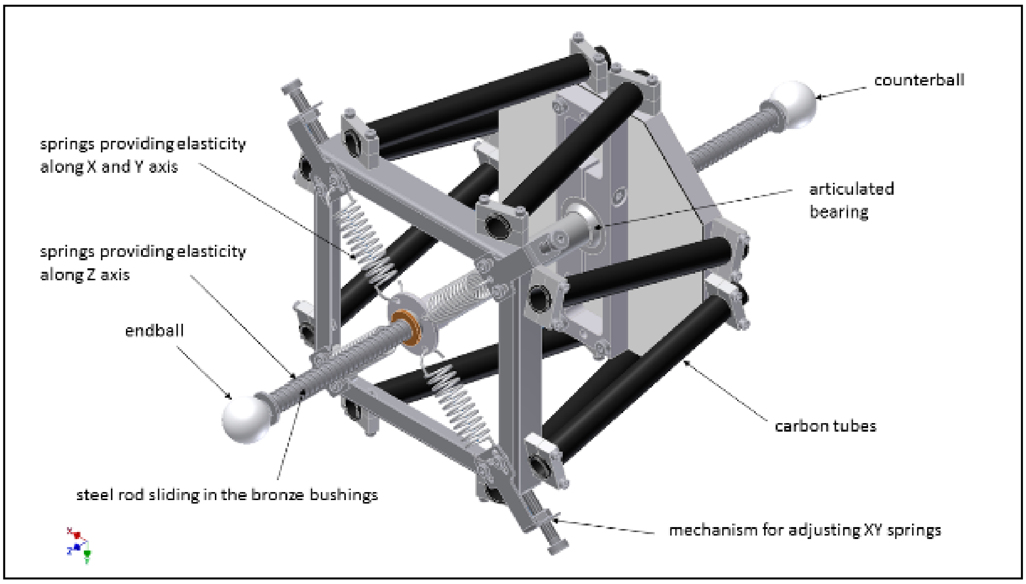


Figure 13: End effector with described the most important elements

## 7. Tests Results

The followed Design, Development, Verification and Validation (DDVV) approach for ORCO is based on the incremental/iterative testing fidelity paradigm (Figure 14) based on the well-known integrated chain FES (Model In the Loop/Functional Engineering Simulator) ➔ SW (Auto)Coding ➔ Real-time (Processor in the Loop, PIL) T/B ➔ HW In the Loop (HIL) T/B.

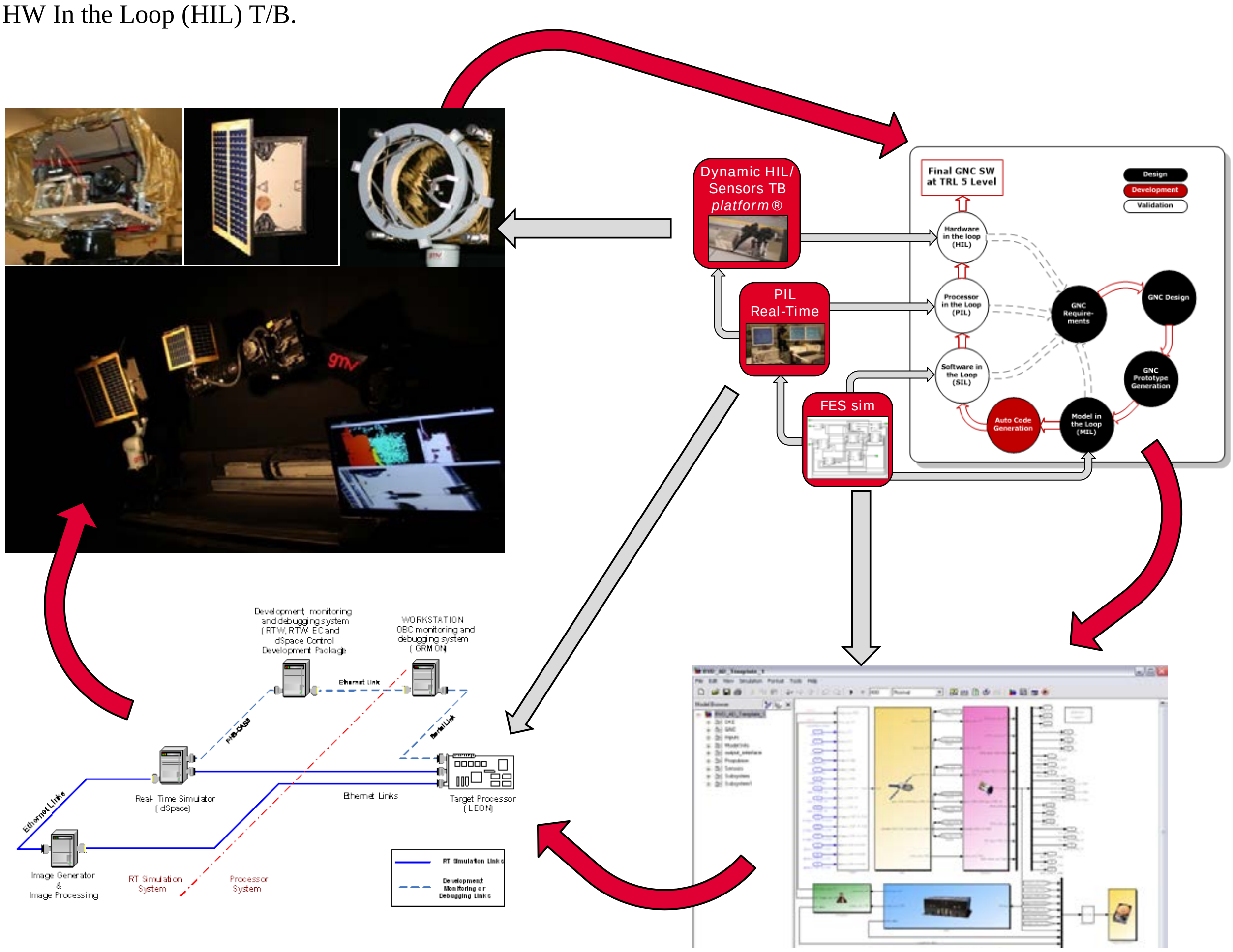


Figure 14: ORCO proposed DDVV incremental/iterative approach

DOI: 10.13009/EUCASS2017-632



### 7.1 Model-in-The-Loop Simulator Results

Some results corresponding to the worst spinning scenario case (#3 in section 2.1) are presented hereafter.

- Figure 15 shows the 3D trajectory followed by the Chaser spacecraft during the test case.
- Figure 16 presents the Image Processing algorithms results. It can be observed that given the highly variable relative orientation between the spacecraft and the illumination direction, the error/uncertainty level is: on the one hand changing along the synchronisation scenario; on the other hand finally dropping to a constant good value when the artificial on-board light is turned on in the last station keeping phase.
- Figure 17 and Figure 18 show in a synthetic way the GNC performance during the final station keeping phase (in LVLH reference frame). Again, the braked arm case (light blue) is superimposed with the moving arm case (dark blue).

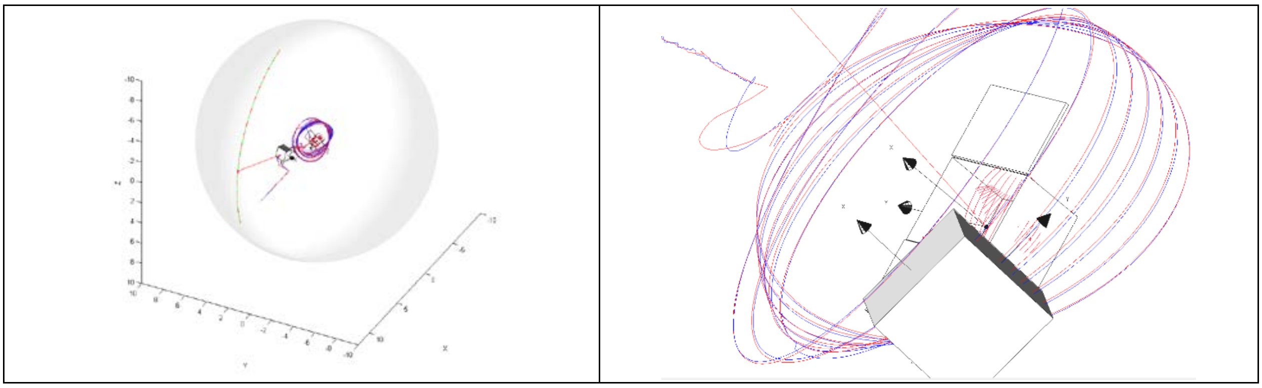

Figure 15: 3D View of the Chaser S/C trajectory (left: synchronisation phase; right: Station keeping)

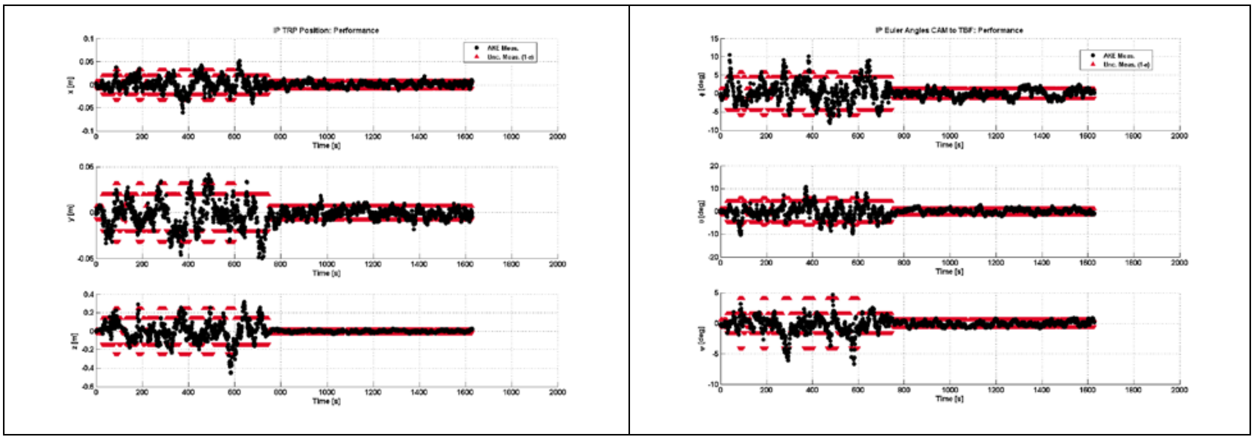

Figure 16: Image Processing Performance (with moving manipulator inducing perturbations)

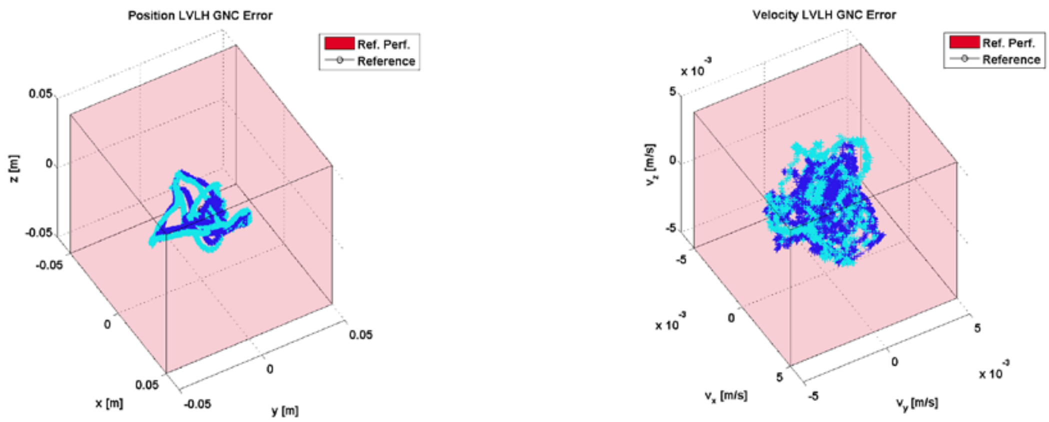


Figure 17: Position (left) and Velocity (right) GNC Error with/without (dark/light blue) LEMUR Operations

DOI: 10.13009/EUCASS2017-632



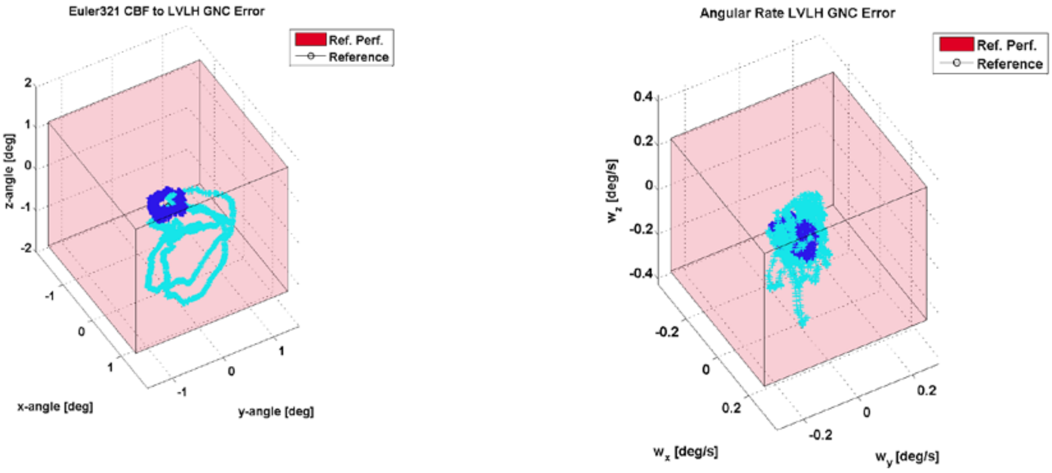


Figure 18: Attitude (left) and Angular Rate (right) GNC Error with/without (dark/light blue) LEMUR Operations

### 7.1 HW-in-The-Loop Simulator Results

The following reported results correspond again to the worst spinning scenario case (#3 in section 2.1).

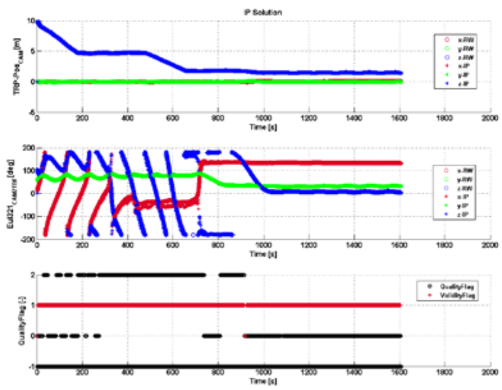

Figure 19: IP Solution and QualityFlag

Figure 19 shows the IP solutions (Target-Reference-Point relative position estimation in Camera Frame and Target Attitude in camera frame as Euler-321 angles) as well as the value of the QualityFlag (black markers) and overall sensor validity flag (red markers) along the entire scenario. It can be observed as the QualityFlag changes between values 2, 1and 0: highlighting the dynamical change of the relative illumination conditions during the HIL scenario.

IP performance are represented in Figure 20 in terms of absolute knowledge error and 1-σ uncertainty. The error has been computed wrt to the simulation real-world value considering a standard delay (consistent with real HPVN Camera and IP algorithm capture, and processing time) of 0.8s.

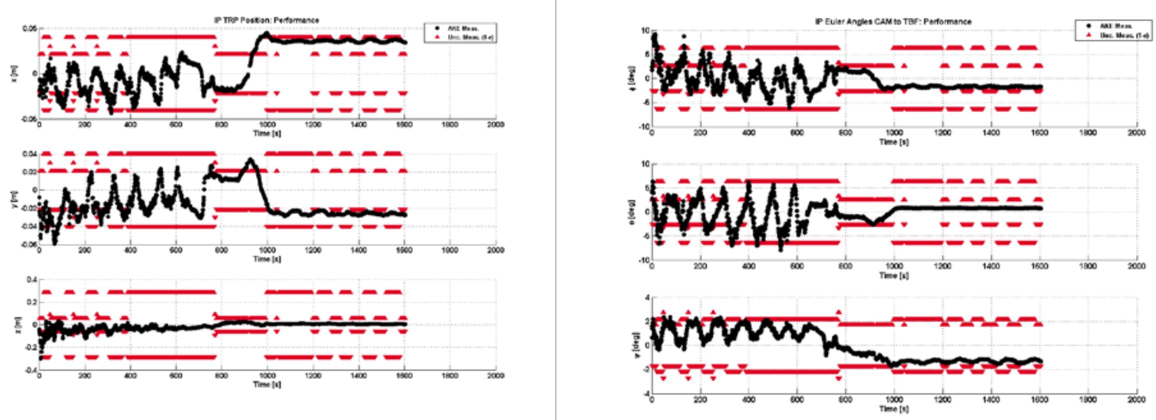

Figure 20: Image Processing Performance (in camera frame)

From the images above it is evident the change of the uncertainty level according to the change of the Quality Flag, and it can also be confirmed the consistency of the error level with the QualityFlag (defining the uncertainty level) itself.

DOI: 10.13009/EUCASS2017-632



Particularly interesting are the periodical components of the error during the first part of the test (while target spacecraft is rotating within the camera frame, till 800s approximately) and the constant biases that can be observed during the SK phase (from about 1000s on) both for translation and attitude IP solution. After different analyses it has been concluded (and measured) that those errors are due to some residual mis-calibration of the laboratory and, mainly, due to the mockup flexibility deformation due to ground gravity effects. For future tests, the mockup flexibility due to ground gravity shall be characterized before the test and removed from the test in real-time by using, for instance, interpolable lookup tables.
This laboratory mis-calibration is affecting to the final GNC performances obtained during HIL tests within ***platform-art***© dynamic test facility. Figure 21 and Figure 22 show the final station keeping phase GNC performance in LVLH frame. It can be seen as the slightly worse navigation performance (wrt simulation and mainly due to laboratory mockup flexibility) are reaching the ~10 cm error cube box, with velocity error slightly exceeding the 5e-3m/s. This biased control error level is already acceptable within the LEMUR limits/requirements to operate safely till contact. Moverover, and in spite of the IP solution bias, the attitude overall performance appears more than acceptable, being the orientation error well under the 1 deg and the angular rate error lower than 1deg/s.

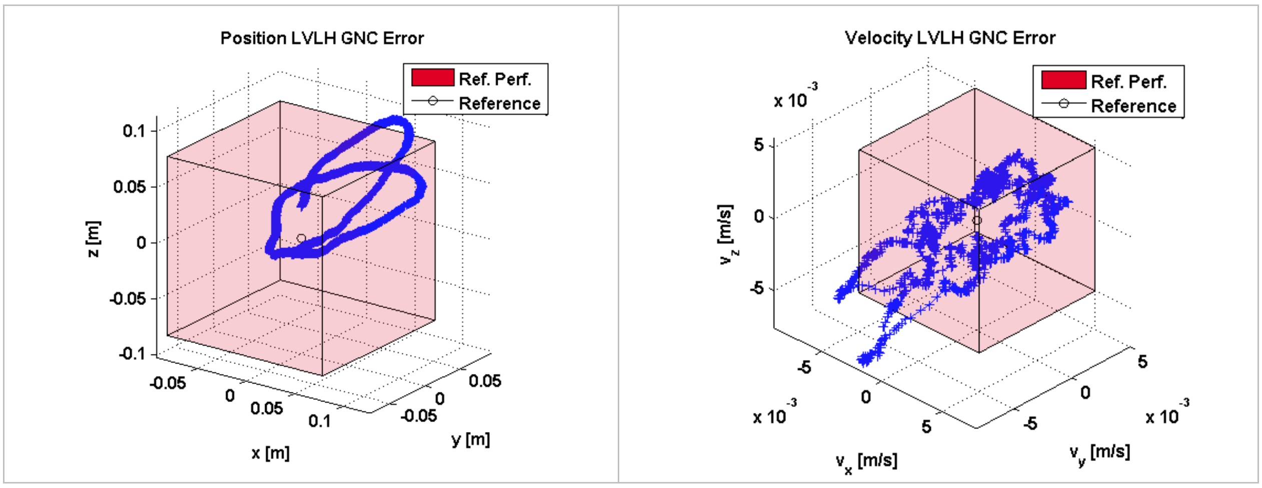


Figure 21: Postion and Velocity GNC Error during Station Keeping

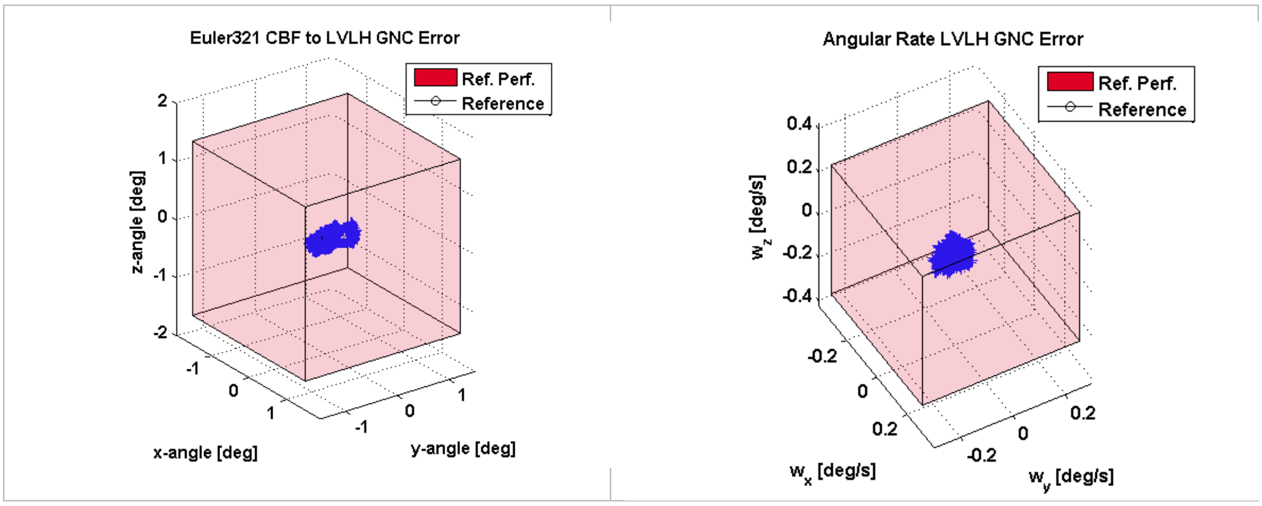


Figure 22: Attitude and Angular Rate GNC Error during Station Keeping

DOI: 10.13009/EUCASS2017-632



## 8. Conclusions

The major ORCO activity conclusions are hereafter summarized:

- The full set of identified critical technologies for In-Orbit Servicing/Active Debris Removal (IOS/ADR) have been significantly worked out/matured during ORCO activity
- Rendezvous and close-proximity operations have been successfully demonstrated with only a vision-based camera as relative navigation sensor assumed that:
    - The navigation filter and the IP have information about the illumination quality (in terms of goodness/badness for IP purposes) ➔ blackouts are solved by propagating previous state (stable target rotation)
    - There is an on-board illumination source that can be used for the very last meters of operations (to avoid blackouts/propagation periods in very high collision risk operations)
- Successful independent operation of chaser SC GNC and robotic manipulator controller has been demonstrated assumed that:
    - There is a-priori knowledge of the intended dynamic (guidance/path planning crossed-knowledge)
    - Force/torque load cell is in the loop for feedback during the contact
- Achieved TRL can be set in:
    - TLR 4/5 for the full system (TRL5 at functional level, TRL4 at interfacing level)
    - TRL 5/6 for the vision-based system (both functional and interfaces) ➔ candidate to be flown as experiment

## References


[1] SoW Active Debris Removal for a small satellite mission (AnDROiD). GSP-SOW-13-700. Issue 1.0. 12/06/2013

[2] Conceptual Design of Active Debris Removal for a Small Satellite mission (AnDROiD). GMV.ANDROID.D1. Issue 1.1. 16/06/2014.

[3] Appendix 1 Statement of Work for the hArmonised System Study on Interfaces and Standardisation of fuel Transfer (ASSIST). ITT/1-7968/14/NL/SFe (SOW). ASSIST - TEC-MMA/2014/133. Issue 1.0. 13/06/2014.

[4] iBoss, DLR presentation at ASTRA 2011, available at: http://robotics.estec.esa.int/ASTRA/Astra2011/Presentations/Plenary%201/07_sommer.pdf . 12/04/2011

[5] H2020 PERASPERA, Master Plan of SRC activities D3.4. Issue 1.0. 30/01/2015